

## Quarkonia at finite temperature in relativistic heavy ion collisions

SAUMEN DATTA<sup>a,\*</sup>

<sup>a</sup>Department of Theoretical Physics, Tata Institute of Fundamental Research, Homi Bhabha Road, Mumbai - 400005, India.

**Abstract.** The behavior of quarkonia in relativistic heavy ion collisions is reviewed. After a detailed discussion of the current theoretical understanding of quarkonia in a static equilibrated plasma, we discuss quarkonia yield from the fireball created in ultrarelativistic heavy ion collision experiments. We end with a brief discussion of the experimental results and outlook.

**Keywords.**  $J/\psi$  suppression, quarkonia, quark-gluon plasma

**PACS Nos.** 12.38.Mh, 12.38.Gc, 25.75.Nq

### 1. Introduction

The connection between quarkonia and deconfinement began with the remarkable paper of Matsui and Satz [1]. The basic idea is extremely simple. At high temperatures, due to Debye screening the binding between a  $\bar{Q}Q$  pair becomes of the Yukawa form, and for sufficiently high temperatures the  $\bar{Q}Q$  meson does not form as the binding becomes sufficiently weak. For  $J/\psi$  the temperature was estimated to be very close to  $T_c$ , the temperature for transition from a hadronic state to a deconfined plasma. Because the  $J/\psi$  shows a prominent peak in the dilepton channel, the disappearance of this peak would be the indicator of deconfinement. In follow-up papers [2, 3], the dissociation temperature of various quarkonia was calculated using the Debye screened form. It was found that the 1S charmonia would decay very close to the transition temperature while the 1P, 2S etc states would decay even earlier. On the other hand, the  $\Upsilon$  was found to survive till much higher temperatures. Therefore the quarkonia states were suggested as a thermometer for the plasma.

A suppression of the  $J/\psi$  peak was indeed found in the fixed target 158A GeV Pb-Pb collisions<sup>1</sup> in the NA50 experiment in CERN [4]. Similar suppression has also been seen in the colliding machine experiments at 200A GeV Au-Au collision in RHIC, and at 2.76A TeV Pb-Pb collisions in LHC.

A more detailed theoretical analysis of the behavior of quarkonia in quark-gluon plasma (QGP), however, has shown more intricacies than originally thought. Even in the case

---

\*saumen@theory.tifr.res.in

<sup>1</sup>Throughout this report, we will be discussing nucleus-nucleus collisions, with a given energy per nucleon. In such cases, the energy will be written as xxxA GeV, where xxx GeV is the energy per nucleon and A is the mass number.

of static equilibrium plasma, theoretically the simplest one to handle, the behavior of quarkonia seems quite complicated in the temperature regime  $1 - 3T_c$  which is of interest to relativistic heavy ion collision experiments. Experimentally, there is strong evidence that a deconfined medium has been formed in relativistic heavy ion collision experiments. While suppression of quarkonia have been a generic feature in these experiments, the detailed behavior has been more complicated to understand. Quarkonia remain among the most studied observables in such experiments; but probably they provide more an insight into the nature of the plasma rather than act as a thermometer.

Here we will review our current understanding of the theory of quarkonia in deconfined medium. In the next section, we will discuss in some detail the idealized problem of quarkonia in an equilibrated plasma at a fixed, not-too-high temperature. In Sec. 3 we will discuss attempts to study quarkonia in the fast expanding fireball that is created in the experiments. Section 4 contains a short outline of the main experimental results, for completeness. The last section contains a summary.

## 2. Quarkonia in static equilibrium plasma

In this section we will discuss our current theoretical understanding of, and challenges in understanding of, the behavior of quarkonia in deconfined plasma. For definiteness, we will consider the case of a  $\bar{Q}Q$  pair in a definite quantum number channel, put in as probe of the medium, where  $Q$  can be charm or bottom.

As outlined in Sec. 1, the first studies of quarkonia in QGP were built on the reasonably successful nonrelativistic potential model approach to quarkonia spectroscopy. Instead of a confining potential, the Debye screened form of the potential,

$$V(r) = -\frac{4}{3} \frac{\alpha_s}{r} e^{-m_D r} \quad (1)$$

was used. Here  $\alpha_s$  is the strong coupling constant and  $m_D$ , the debye mass in QGP. The aim was to calculate a dissociation temperature for the different quarkonia by solving the Schrödinger equation with  $V(r)$ . The perturbative form of the potential was later substituted by the free energy of a static  $\bar{Q}Q$  pair, calculated from lattice.

Use of Eq. (1) in this way, however, is not based on strong theoretical footing. Recent attempts to understand the behavior of quarkonia in-medium have started with a rephrasing of the question: e.g., “what happens to the  $J/\psi$  peak in the dilepton channel if a plasma is formed?” is best understood by looking at a quantity that directly looks at the dilepton channel.  $J/\psi$  connects to the dilepton channel by the point vector current  $V_i(x) = \bar{c}(x)\gamma_i c(x)$ , and the suitable correlator of this current controls the dilepton rate. The dilepton rate can be directly connected to the spectral function, which is the fourier transform of the correlator, [5]

$$\rho_H(p_0, \vec{p}) = \int dt \int d^3x e^{ip_0 t - i\vec{p}\cdot\vec{x}} \langle [J_H(\vec{x}, t), J_H(\vec{0}, 0)] \rangle \quad (2)$$

where  $J_H(\vec{x}, t) = \bar{Q}(\vec{x}, t)\gamma_H Q(\vec{x}, t)$  is the suitable hadronic point current, and the angular bracket indicates thermal averaging.  $\rho_H(p_0, \vec{p})$  is called the spectral function and is proportional to the dilepton rate.

A mode expansion of  $\rho_H(p_0, \vec{p})$  is instructive. Inserting a complete set of states, one can write  $\rho_H(p_0, \vec{p})$  as

$$\rho_H(p_0, \vec{p}) = \frac{1}{Z} \sum_{n,m} \left( e^{-k_n^0/T} - e^{-k_m^0/T} \right) |\langle n | J_H(0) | m \rangle|^2 \delta^4(p^\mu - k_m^\mu + k_n^\mu) \quad (3)$$

where the sum over states includes both discrete and continuous states, and  $k_n^\mu$  is the four-momenta of the state  $|n\rangle$ .

In case of a free scalar particle of mass  $M$ , the expression above leads to a spectral function

$$\rho_H(p_0, \vec{p})|_{\text{free}} = \epsilon(p_0) \delta(p^2 - M^2). \quad (4)$$

As  $T \rightarrow 0$ , a stable meson contributes a similar term to the spectral function in QCD (with a multiplicative factor  $|\langle 0 | J_H | M \rangle|^2$ ). When the state is unstable, the delta function gets smeared into a smooth peak, whose width reflects the decay width of the particle. For a particle like the  $J/\psi$  with a narrow decay width, one gets an almost- $\delta$  function peak, which shows up in the dilepton cross section. At finite temperatures, as Eq. (3) shows, we will have a more complicated expression; the question of interest is whether the peak structures corresponding to various quarkonia survive at a given temperature.

### 2.1 Spectral function using lattice QCD

QCD, the theory of strong interactions, cannot be directly defined on the continuum (like other quantum field theories), and needs to be regularized. Regularization using a space-time lattice has proved invaluable for studies of the nonperturbative regime of QCD, as one can use numerical Monte Carlo techniques. Much of our current knowledge of strongly interacting matter at moderately high temperatures (that are of interest to the ultrarelativistic heavy ion collision experiments), in particular the transition temperature, equation of state, nature of the transition, etc, comes from lattice QCD [6].

Since we are interested in the spectral function,  $\rho$ , at temperatures  $\lesssim 3T_c$ , where perturbation theory may not work very well, it would be ideal to calculate the spectral function,  $\rho(\omega = p_0, \vec{p})$  using lattice QCD. The catch is that lattice QCD is defined in Euclidean time, and the thermal correlators one can calculate numerically are the Matsubara correlators

$$C_H(\vec{x}, \tau) = \langle J_H(\vec{x}, \tau) J_H(\vec{0}, 0) \rangle \quad (5)$$

where  $\tau \in [0, \beta = 1/T)$  is defined in the Euclidean time direction. In order to get the real time correlators of Eq. (2) one needs to use an analytic continuation in time,  $\tau \rightarrow -it$ . This leads to the following integral equation connecting  $\rho_H(\omega, \vec{p})$  and  $C_H(\vec{x}, \tau)$ :

$$C_H(\tau, \vec{p}) = \int d^3x e^{-i\vec{p}\cdot\vec{x}} C_H(\vec{x}, \tau) = \int d\omega \rho_H(\omega, \vec{p}) K(\omega, \tau) \quad (6a)$$

$$K(\omega, \tau) = \frac{\cosh \omega(\tau - 1/2T)}{\sinh \omega/2T}. \quad (6b)$$

For  $T = 0$ , Eq. (6a) simplifies to a Laplace transform. In the rest of this section, we will mostly consider correlators projected to  $\vec{p} = 0$ , and denote them simply as  $C_H(\tau)$ , omitting the  $\vec{p}$  argument. The corresponding spectral function  $\rho_H(\omega, \vec{p} = 0)$  will be written as  $\rho_H(\omega)$ .

The first lattice studies of  $J/\psi$  and other charmonia states are about a decade old [7–9]. They all used the “quenched approximation”, i.e., the plasma was purely gluonic.  $\mathcal{O}(10)$  (12-32) data points were used in the  $\tau$  direction, and the spectral function was estimated using Eq. (6a). An examination of Eq. (6a) immediately shows the difficulty of the extraction of  $\rho_H(\omega)$  from  $C(\tau)$ : the inverse Laplace transform is a very nontrivial problem numerically, made even more difficult by the dual facts of the small range of  $\tau$  at high temperatures and the  $\mathcal{O}(10)$  data points. Note that because of the periodicity of the kernel in Eq. (6b), one has independent information about Matsubara correlation only for  $\tau \in [0, \beta/2)$ . Clearly, a direct inversion of Eq. (6) is not possible. The studies used the maximum entropy method (MEM) [10], where Bayesian theory is used to provide information about the solution  $\rho_H(\omega)$  when it is not constrained by the data. If one treated the extraction of  $\rho_H(\omega)$  from  $C(\tau)$  as, e.g., a simple  $\chi^2$  minimization problem, one would have many flat directions in the parameter space. In maximum entropy method, one stabilizes the analysis by recasting it as a maximization of the combination

$$\mathcal{L} = -\frac{1}{2} \chi^2 + \alpha S, \quad (7a)$$

$$S = \sum_i \Delta\omega_i \left( \rho_H(\omega_i) - \rho_0(\omega_i) - \rho_H(\omega_i) \log \frac{\rho_H(\omega_i)}{\rho_0(\omega_i)} \right). \quad (7b)$$

Here  $\rho_0(\omega)$  is the default solution provided as an input to the analysis; in the absence of data, Eq. (7) implies that  $\rho_H(\omega) = \rho_0(\omega)$ . Eq. (7b) has the form of entropy in information theory, giving the method its name. Given a set of  $C(\tau)$  the maximization of  $\mathcal{L}$ , Eq.(7a), has a unique solution [10]. Note that this by itself does not guard against a solution unstable against noise. As pointed out by Bryan [11], parametrized suitably, the solution space can be restricted to the space spanned by singular directions [12] of the kernel in Eq. (6a), whose dimensionality is no more than the number of data points.

While the early studies, Ref. [7–9], differed in some details, they all found that the spectral function of  $J/\psi$  was not very sensitive to the phase transition: the changes in  $\rho_H(\omega)$  were small as one crossed  $T_c$ . A clear peak structure was found even at  $1.5 T_c$ . In addition, the dissolution of the peak was found to be gradual rather than abrupt [7, 8], with a broadening and weakening of the peak as one went to higher temperatures. On the other hand, the 1P states ( $\chi_c$ ) were seen to change much more abruptly across the transition. The spectral functions calculated in Ref. [7] for the scalar,  $\bar{c}c$ , and vector,  $\bar{c}\gamma_i c$ , operators are shown in the left panel of Fig. 1. The correlators  $c(\tau)$  show very little change in the vector channel as one crosses  $T_c$ , even upto  $1.5 T_c$ ; this resulted in an extracted spectral function that showed a strong  $J/\psi$  peak even at  $1.5 T_c$ . On the other hand,  $C(\tau)$  in the scalar channel showed serious modification on crossing  $T_c$ , and major weakening of the  $\chi_{c0}$  peak was seen already at  $1.1 T_c$ . Several follow-up studies reached qualitatively similar conclusions [13]. Also a dynamical study with 2-flavor QCD (but with a somewhat heavy pion) found very similar results, when temperatures are expressed in units of  $T_c$  [14]. A very recent dynamical study, again with a somewhat heavy pion, has also found very little change in the 1S state peaks upto temperatures  $\sim 1.4 T_c$  [15].

On the other hand, the systematics of the inversion of Eq. (6) is large, and probably the extraction of  $\rho_H(\omega)$  was less reliable than what the convergence of the different results suggested. In particular, it was pointed out later that a large part of the change in the 1P channels is due to the diffusion peaks in these channels [16]. The free spectral function in the vector, axial vector, and scalar channels have a contribution

$$\rho_H(\omega) \xrightarrow{\omega \rightarrow 0} 2\pi \chi_H(T) \omega \delta(\omega) \quad (8)$$

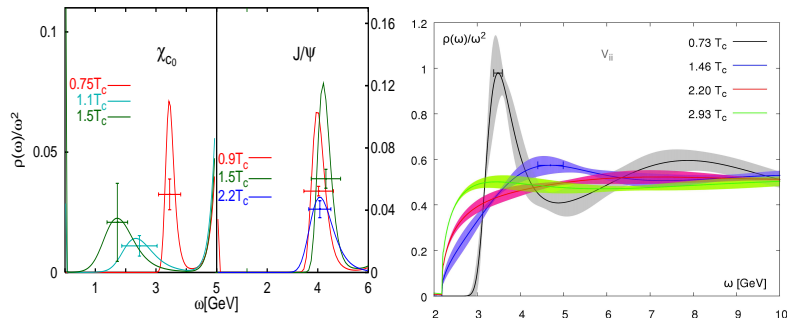


**Figure 1.** (Left) Spectral functions of the  $\bar{c}c$  and  $\bar{c}\gamma_i c$  operators from Ref. [7], showing the modification of the  $\chi_{c0}$  and survival of the  $J/\psi$  peak after deconfinement. The vertical error bar indicates the error for the reconstructed spectral function, averaged over the  $\omega$  range indicated by the horizontal band [10]. (Right) Spectral function of the  $\bar{c}\gamma_i c$  operator ([19], ©American Physical Society) showing serious modification of the  $J/\psi$  peak already below  $1.5 T_c$ . The band is the error estimate from a simple jackknife analysis.

which contribute an additive constant to  $C(\tau)$ . In the interacting theory the  $\delta$  function becomes a smooth peak, leading to a near-constant term in the correlator. It has been shown [16, 17] that much of the change in the 1P channel correlators comes from this low- $\omega$  contribution. It was also pointed out that even at small temperatures  $T \sim 0$ , when one restricts oneself to a small range in Euclidean time, it is difficult to isolate the peak structure from Euclidean correlator data [13]. In a series of papers Mocsy and Petreczky [18] have shown that the lattice data of  $C(\tau)$  is also consistent with a large change in the peak structure at relatively smaller temperatures.

A recent study, similar in approach to Refs. [7, 9] but using finer lattices [19], has found that even in the vector and pseudoscalar channels, the peak structure is considerably softened already at  $1.5 T_c$ . Results from this study are also shown in the right panel of Fig. 1. It is to be understood that the analysis is similar to the earlier lattice studies, and can suffer from similar systematic effects as those. While it is certainly reasonable to hope that lattice QCD will be able to provide the spectral function with much better systematics in the future, it would be important to incorporate new ideas into the calculation.

In the bottomonia sector, there have been interesting recent studies [20, 21] using the formalism of non-relativistic QCD (NRQCD) on lattice [22]. Use of NRQCD has two advantages in this context. In NRQCD the heavy quark mass  $m_Q$  is much larger than all other scales, and one replaces  $\omega$  in Eq. (6b) by  $2M_Q + \omega$ . Then for  $M_Q \gg T$ , one replaces the periodic kernel Eq. (6b) by a simple exponential,  $\exp(-\omega\tau)$ . Therefore independent correlator data is now available for the whole range  $[0, \beta)$ . Also since one is now studying only excitations around  $2M_Q$ , the low- $\omega$  diffusion peak structure is absent. Ref. [20] calculated the correlators in this formalism, and applied Bayesian analysis, Eq. (7), to extract  $\rho_H(\omega)$ . They found that 1S bottomonia survive at least till temperatures of  $2 T_c$ ; see Fig. 2. On the other hand, the 1P peaks were found to dissolve right after  $T_c$  [21]. These results are qualitatively in agreement with earlier, preliminary studies of bottomonia within the relativistic framework [23].

The peak position and the decay width of the 1S states have also been extracted from the NRQCD studies of the Euclidean correlator in Ref. [20]. The decay width,  $\Gamma$ , calculated

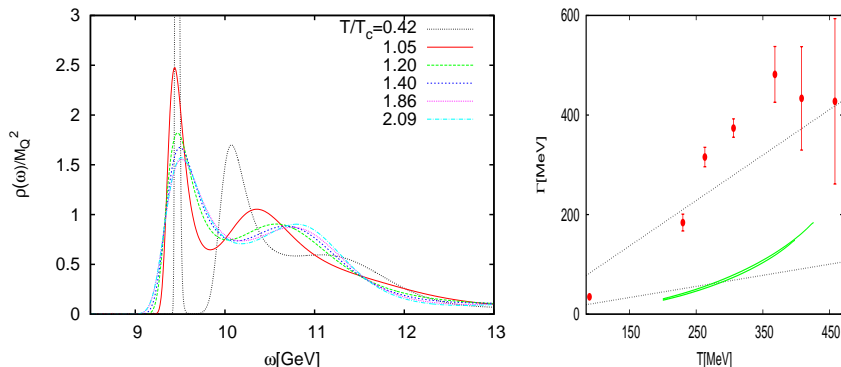


**Figure 2.** (Left) Spectral function of the  $\bar{b}\gamma_\mu b$  current at various temperatures, extracted from lattice correlators [20]. A strong peak for  $\Upsilon(1S)$  survives even at  $\sim 2T_c$ . (Right) Width of the  $\Upsilon(1S)$  peak at various temperatures, extracted from lattice correlators [20]. Also shown are (green, solid line) results of a calculation from HTL potential (see Sec. 2.2 and Fig. 3), and (black, dotted line) the trend from leading order of perturbation theory [20, 24] for  $\alpha_s = 0.25$  (lower line) and 0.4 (upper line).

in Ref. [20], is also shown in Fig. 2 (for their system,  $n_f = 2$  with  $m_q$  close to the strange quark mass,  $T_c$  is estimated to be  $\sim 220$  MeV). A near-linear increase of  $\Gamma$  with temperature is seen. It is interesting to note that in effective field theory calculations at weak coupling and  $\alpha_s m_Q \gg T$ ,  $\Gamma \sim 14 \alpha_s^3 T$  in leading order [20, 24]. Within the rather large systematics, the lattice data is roughly in agreement with this for  $T \gtrsim 250$  MeV, for  $\alpha_s \sim 0.4$ . Note that Fig. 2 indicates a large decay width for the 1S bottomonia already above  $T_c$ . The origin of such a decay width would be collisions with the thermal quarks and gluons in the medium. Of course, the systematic error associated with the extraction of width from the Euclidean correlator is large, and Ref. [20] suggests that the calculated widths should be treated as an indicative upper limit. Preliminary results from another study, which also uses NRQCD formalism to calculate bottomonia correlators, has reported much smaller widths at comparable temperatures [25].

While lattice NRQCD provides a very promising way to study bottomonia in medium, it is fair to say that the studies are still reasonably recent and various systematics need to be better examined.

## 2.2 Nonrelativistic approach and “potential at finite $T$ ”

A direct extraction of the spectral function from correlation functions calculated in lattice QCD is the most direct approach to understanding the behavior of quarkonia in deconfined plasma. Unfortunately, as discussed in the previous section, at the moment the systematics of such a study are not in complete control. This is likely to change with time. However, it will surely help to supplement this direct approach with insights gained from other studies.

A nonrelativistic potential approach has been remarkably successful in quarkonia spectroscopy; it is therefore natural that several attempts have been made to extend such an approach to finite temperatures. The first step towards this was the identification of the free energy cost of putting an isolated  $\bar{Q}Q$  pair in a thermal medium [26]. As the distance between the  $Q$  and the  $\bar{Q}$  increases, in the confined medium the free energy cost of in-

roducing such a pair also increases. As  $m_Q \rightarrow \infty$ , the quark is static and the effect of such a quark is approximated by a phase factor  $\sim e^{-m_Q \beta}$  multiplying a timelike gauge connection, called a Polyakov loop,  $L$ , defined as

$$P(x) = \prod_{i=0}^{N_\tau-1} U_0(\vec{x}, i) \quad (9a)$$

$$L(x) = \text{Tr } P(x). \quad (9b)$$

After suitable mass renormalizations, one can define the free energy cost mentioned above:

$$\mathcal{F}_{\bar{Q}Q}^{\text{av}}(\vec{x}) = \log \langle L(x) L^\dagger(0) \rangle \quad (10)$$

Note that  $L(x)$  is invariant under color rotations, and therefore, the free energy defined in Eq. (10) includes an averaging over the color orientations of the  $Q$  and  $\bar{Q}$ . If one wants to study a  $Q$  and  $\bar{Q}$  in a singlet combination, as in quarkonium, it can be defined using  $P(x)$ , Eq. (9a) [27]:

$$\mathcal{F}_{\bar{Q}Q}^{\text{sing}}(\vec{x}) = \log \langle \text{Tr } P(x) P^\dagger(0) \rangle \quad (11)$$

The right hand side in the above equation is not gauge invariant, and therefore, needs to be calculated after fixing to a gauge. In perturbation theory, it can be shown that  $\mathcal{F}_{\bar{Q}Q}^{\text{sing}}(\vec{x})$  is gauge invariant, and in leading order, has the expression

$$\mathcal{F}_{\bar{Q}Q}^{\text{sing}}(\vec{x}) = -\frac{4}{3} \frac{\alpha_s}{r} e^{-m_D r}. \quad (12)$$

It has been evaluated also nonperturbatively, using Eq. (11) in the Coulomb gauge [28].

$\mathcal{F}_{\bar{Q}Q}^{\text{sing}}(\vec{x})$  has been widely used in the literature to study the fate of quarkonia in QGP, by using it as a finite temperature potential; it denotes, though, a free energy, and not a potential. There has been considerable effort over the last decade towards constructing a suitable potential for quarkonia at finite temperature, in a field-theoretic framework [29–31]. In vacuum, the effective field theoretic framework for formally defining such a potential relies on the hierarchy of scales,  $m_Q \gg m_Q v \sim 1/r \gg E_b \sim m_Q v^2 \sim g^2/r$ , where  $v \ll 1$  is the relative velocity of the heavy quark,  $Q$ , and antiquark,  $\bar{Q}$ , in the bound state, and  $E_b$  is the binding energy. The idea is to write down an effective theory containing only the degrees of freedom relevant for  $\bar{Q}Q$  near threshold, i.e., those at scale  $E_b$ . So scales of  $m_Q$  and  $m_Q v$  are integrated out. Integrating out of the scale  $m_Q$  leads to standard non-relativistic QCD (NRQCD), while further integrating out  $m_Q v$  leads to so-called potential NRQCD (pNRQCD) [32], with Lagrangian

$$\begin{aligned} \mathcal{L}_{\text{pNRQCD}} = & S^\dagger(\vec{r}) \left( i\partial_0 - \frac{p^2}{2m_Q} - V_S(r) + \text{corr.} \right) S(\vec{r}) \\ & + O^\dagger(\vec{r}) \left( iD_0 - \frac{p^2}{2m_Q} - V_O(r) + \text{corr.} \right) O(\vec{r}) + \dots \end{aligned} \quad (13)$$

where  $S, O$  denote the  $\bar{Q}Q$  in singlet and octet representations, respectively, and  $V_{S,O}$  denote the corresponding potentials. The ... include the singlet-octet transition terms. For sufficiently heavy quarks such that  $m_Q v \gg \Lambda_{\text{QCD}}$ , the parameters of  $\mathcal{L}_{\text{pNRQCD}}$  can be obtained perturbatively.

At finite temperatures, a new set of scales related to the temperature  $T$  are introduced. At very high temperatures, one can write down a hierarchy  $T \gg m_D \sim gT \gg g^2T$ , where  $m_D$  is the scale of screening of static charges and  $g^2T$  is the inherently nonperturbative magnetic scale. Integrating out the scale  $T$  leads to the standard HTL (hard thermal loop) Lagrangian [33]. The form of the finite temperature potentials depend on the relative hierarchy of the thermal scales and the scales related to  $m_Q$  [30].

Let us take  $m_Q \gg T \gg m_Q v$ . Integrating out  $m_Q$  and  $T$  then leads to the HTL version of NRQCD. If  $m_Q v \sim m_D$ , integrating out these scales leads to a potential which was first derived in Ref. [29] slightly differently. The spectral function relevant to the dilepton peak is connected to the fourier transform of the real-time correlator

$$C^>(t, \vec{x}) = \int d^3x \langle J^\mu(t, \vec{x}) J_\mu(0, \vec{0}) \rangle \quad (14)$$

where  $J^\mu(t, \vec{x})$  is the point vector current defined after Eq. (2). Replacing  $J_\mu$  in Eq. (14) by a point-split current

$$J_\mu^{\text{split}}(t, \vec{x}; \vec{r}) = \bar{\psi} \left( t, \vec{x} + \frac{\vec{r}}{2} \right) \gamma_\mu U \left( t; \vec{x} + \frac{\vec{r}}{2}, \vec{x} - \frac{\vec{r}}{2} \right) \psi \left( t, \vec{x} - \frac{\vec{r}}{2} \right) \quad (15)$$

it is easy to check that in the non-interacting theory for non-relativistic quarks,  $C_{\text{split}}^>(t, \vec{x}; \vec{r})$  satisfies a Schrödinger-like equation

$$\left( i\partial_t - \left( 2m_Q - \frac{\nabla_r^2}{2m_Q} \right) \right) C_{\text{split}}^>(t, \vec{x}; \vec{r}) = 0 \quad (\text{to } \mathcal{O}(1/m_Q^2)). \quad (16)$$

In the interacting theory, one can define a potential by equating the left hand side of Eq. (16) to  $V(t, \vec{r}) C_{\text{split}}^>(t, \vec{x}; \vec{r})$ . Taking the static limit,  $m_Q \rightarrow \infty$ , one gets

$$i\partial_t W(\vec{r}, t) = V(\vec{r}, t) W(\vec{r}, t). \quad (17)$$

where  $W(\vec{r}, t)$  is the timelike Wilson loop. Going to the long time limit leads to

$$\begin{aligned} V(r) &= -\frac{4}{3}\alpha_s \left( \frac{e^{-m_D r}}{r} + m_D \right) - i\frac{8}{3}\alpha_s T \Phi(r) \\ \Phi(r) &= \int_0^\infty \frac{dz z}{(z^2 + 1)^2} \left( 1 - \frac{\sin zr}{zr} \right) \end{aligned} \quad (18)$$

in leading order HTL approximation [29, 30].

While for the plasma created in RHIC and LHC, the validity of the weak coupling approximation used in reaching Eq. (18) is questionable, it is instructive to examine some features of the potential. The real part of  $V(r)$  is, modulo a constant, identical to the debye-screened singlet free energy in Eq. (12). Interestingly, there is also an imaginary part to the potential. The imaginary part leads to a thermal width  $\propto \alpha_s T$  of the spectral function peak, which incorporates the physics of Landau damping [34]. To get an idea of its contribution, Ref. [29] treated the imaginary part as a perturbation, to get the decay width. For  $\Upsilon$  it was found that already at not-too-large temperatures  $\sim 250$  MeV, while the bound state survives, it acquires a considerable thermal width (see Fig. 3). This thermal width, though, is smaller than that extracted in Ref. [20] from lattice correlators (see Fig. 2).

$V(r)$  (eq.18) was also used to calculate the spectral function, which is simply related to the Fourier transform of  $C^>(\vec{r} \rightarrow 0, t)$  [39]. It was found that for quarks in the bottom mass region, the spectral function peak is severely depleted and broadened already by



$T \sim 350$  MeV, and by a temperature of 450 MeV, no significant peak is visible (see Fig. 3). If one uses the potential for charmonium (where the separation of scales required is highly questionable), one finds that already at  $T \sim 250$  MeV the peak structure is essentially absent. A similar study was also carried out in Ref. [40], where also various systematics were studied. The basic results are similar to Ref. [39]. Also the later study highlighted the major role played by the imaginary part of the potential in broadening the peak. Ref. [40] also calculated the Euclidean correlators, and found that they do not completely agree with the bottomonia correlators obtained from lattice.

As already mentioned, the hierarchy  $T \gg m_Q v$  is not valid at the temperatures of interest in RHIC and LHC. At least for the  $\Upsilon$ , one in fact expects  $m_Q v \gg T$ . In such a case, one first integrates out the scale  $m_Q v$  from NRQCD, to get the pNRQCD action, Eq. (13). Further integrating out the scale  $T$  then leads to thermal corrections which are very different from Eq. (18) [30]. If  $m_D \gg E_b$ , the thermal potential is still well-defined, but the real part of the potential does not have the screened form. The potential still gets an imaginary component, which now has two main components: a term  $\propto \alpha_s^3 T$  which comes from a transition to color-octet state, and terms like  $\alpha_s T m_D^2 r^2$  which are related to Landau damping. On the other hand, if  $E_b \gg m_D$ , the thermal potential is not well-defined. Of course, thermal corrections to the binding energy and the the decay width are well-defined quantities, and have been calculated in weak coupling [24]. The thermal decay width once again has contributions  $\propto \alpha_s^3 T$  related to singlet-to-octet transition, and terms  $\propto \alpha_s T m_D^2 r_0^2$  related to Landau damping [24], where  $r_0 = 3/(2\alpha_s m_Q)$  is the Bohr radius.

One message to take, both from the effective field theory studies and from studies of the previous section, is that even before the dissolution of the quarkonia peak, the states can get a substantial thermal decay width. Rather than a single “dissolution temperature”, it is the temperature-dependent width which is of phenomenological significance. The decay width obtained from the imaginary part of the potential has been compared to phenomenological estimates of quarkonia dissociation in Ref. [34].

In the discussion so far, we have stressed that the imaginary part of the “potential” is a theoretical tool to describe the broadening of the quarkonium structure in the spectral function, due to interactions with the thermal gluons and quarks. Its interpretation has been further clarified using the language of open quantum systems [35, 36]. Starting from a complete description of the  $\bar{Q}Q$  + thermal medium, one can integrate out the thermal medium to get an effective description of the  $\bar{Q}Q$  system in medium. Integrating out of the medium leads to noise terms in the description of the  $\bar{Q}Q$  system, which cause both dissipation of the heavy quark, and a lack of coherence between the  $\bar{Q}Q$  pair in quarkonia, leading to an increased thermal width. This has been worked out in perturbation theory, to give the same complex potential as above [36].

One can also try to calculate the potential, Eq. (17), nonperturbatively, without assuming weak coupling or any particular ordering between the scales  $T$  and  $m_Q v$ . Ref. [37] calculated the Euclidean timelike Wilson loop,  $W(\vec{r}, \tau)$ , and then employed an analytic continuation similar to that described in Sec. 2.1 to obtain the potential from it. A Bayesian analysis similar to, but not identical to, MEM was used [38], which probably needs careful examination by others. A complex potential was extracted from the Euclidean Wilson loop calculated in a gluon plasma. At  $2.33 T_c$ , both the real and the imaginary parts of the potential extracted from the data are considerably different from the hard thermal loop calculation. Note that the timelike Wilson loop is identical to the Polyakov loop correlator in Eq. (11), calculated in the axial gauge. Ref. [37] also calculated the Polyakov loop correlator in Coulomb gauge. Analyzing it in the same way,

they obtained a potential which is much closer to the perturbative calculation of Ref. [29]. Note however that the coulomb gauge calculation was done in great detail already [28]; it is not clear how sensitive the correlation function is to the imaginary part of the potential.

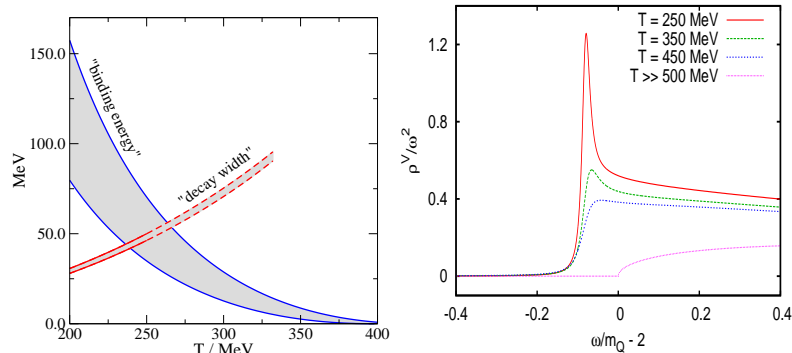


**Figure 3.** (Left) Binding energy and decay width of the  $\Upsilon$  peak in the spectral function of the current  $\bar{b}\gamma_i b$ , using the leading order HTL-resummed potential. From Ref. [29]. (Right) Spectral function calculated directly from the same potential [39]. Here  $m_Q = 4$  GeV.

### 3. Prediction for quarkonia production in relativistic heavy ion collision

In the previous section, we discussed various calculations that investigate the fate of a quarkonium put as a probe in static, equilibrated QGP. Of course, the experimental situation is very different. A  $\bar{c}c$  pair gets formed, probably in a hard collision at early times; the quarkonium state gets formed, either in the pre-equilibrium stage or in the plasma. Also the system is not static, the temperature profile changes. While understanding the behavior of an external  $J/\psi$  in static plasma forms the first step to predicting the  $J/\psi$  production in relativistic collisions, one needs to put it in the context of the fireball created in a heavy ion collision. In this section we discuss some calculations towards quantitative prediction for  $J/\psi$  production in heavy ion collision, and describe some ingredients for such a calculation.

#### 3.1 “Regeneration” and thermal quarkonia

The spirit of the discussion of Sec. 2 was that the  $J/\psi$  is formed very early in the plasma, in a way possibly similar to that in a  $pp$  collision, and we investigate the survival probability of the  $J/\psi$  in the QGP. The hadrons made of light quarks, on the other hand, are described very well by the assumption that as the medium cools to below deconfinement, the quarks present in the medium coalesce to form hadrons according to a thermal distribution. If the density of  $c, \bar{c}$  is sufficiently high in the medium, one also needs to investigate the possibility that at freezeout a  $c$  and a  $\bar{c}$  coalesce to form a  $J/\psi$  [41]. In the literature,  $J/\psi$  production this way is dubbed “regeneration”.

In regeneration calculations [41, 42], the different hadrons with (open or hidden) charm are distributed statistically, just as the light hadrons are. The charm quarks are produced as  $\bar{c}c$  pairs in initial hard collisions, but then will develop in the plasma as colored  $c(\bar{c})$  quarks. At the time of freezeout, they then hadronize according to a statistical thermal

distribution. So the ratios of, e.g., different charmonia will follow a statistical distribution. An early motivation was the fact that the ratios of the production cross-section of the  $\psi'$  and the  $J/\psi$  in the 158A GeV Pb-Pb collisions in SPS followed a statistical distribution [41].

The number of  $J/\psi$  produced will be given as

$$N_{J/\psi} = g_c^2 V n_{J/\psi}^{\text{th}}(T_{\text{fr}}, \mu_B), \quad (19)$$

$$\text{where } n_i^{\text{th}} = g_i \int \frac{d^3p}{e^{(E_i(p)-\mu_i)/T} \mp 1} \quad (20)$$

is the thermal (Bose/Fermi) distribution function for hadron  $i$ ,  $T_{\text{fr}}$  and  $\mu_B$  are the chemical freezeout temperature and baryon chemical potential,  $V$  is the fireball volume, and  $g_c$  is an extra degeneracy factor to take into account the fact that the production of the charm quarks happen in hard collisions and the total number of charm quarks is much larger than it would have been if the charm quarks were chemically equilibrated in the plasma [41].

The model is simple, and with clear predictions for rapidity and  $p_T$  distributions of the  $J/\psi$ . The earlier works on this model [41] found good agreement of the relative yields of  $J/\psi$  and  $\psi'$  in the highest energy Pb-Pb runs of SPS. More recent studies [42] have also found good agreement of this ratio in RHIC. The early studies [41] had also predicted little or no suppression of  $J/\psi$  production in RHIC, and substantial enhancement in LHC, compared to scaled  $pp$  collision results. This has not been borne out by data. More detailed recent studies [42], which take into account the possibility that even in collisions that lead to a plasma in the core, there may be hard collisions between (surface) nuclei which do not lead to plasma formation, have reported good agreement with RHIC data for  $J/\psi$  production.

A generic prediction of the regeneration calculations is more suppression in the forward rapidity region than in midrapidity. This is in qualitative agreement with the trend seen in 200A GeV Au-Au collisions in RHIC. Also, as Eq. (20) suggests, the  $p_T$  distribution will be rather steep. Assuming same  $T_{\text{fr}}$  as light hadrons, a much steeper  $p_T$  distribution is predicted than seen in the experiment [42]. A much larger freezeout temperature  $\sim 360$  MeV, compared to the initial temperature, was required in Ref. [42] to describe the  $p_T$  dependence in RHIC.

A variant of the regeneration mechanism has been suggested in Ref. [43]. In their picture, while the initially produced  $\bar{c}c$  pair does not lead to a  $J/\psi$  formation in the plasma, they do not become completely decorrelated. The motion of a heavy quark in plasma can be understood as a diffusion process [44, 45], with a rather small diffusion coefficient [45, 46]. The smallness of the diffusion coefficient, combined with the interaction between the  $\bar{c}c$  pair, lead to the  $c$  and  $\bar{c}$  staying spatially correlated through their evolution in the fireball. This, the authors argue, leads to a  $J/\psi$  cross-section larger than a naive regeneration calculation suggests, and a  $p_T$  distribution similar to that of the original  $\bar{c}c$  pair.

Some authors (e.g., [47]) have used a combination of directly produced and recombined  $J/\psi$  to explain the  $J/\psi$  yield, e.g., in RHIC. In [47], the  $J/\psi$  yield in SPS is almost completely directly produced. In RHIC, because of the hotter and larger fireball, a larger fraction of the directly produced  $J/\psi$  is suppressed, but some  $J/\psi$  are regenerated, giving a final suppression factor similar to SPS.

Another intuitive signature of regeneration would be elliptic flow of  $J/\psi$  [48]. The charm quark shows substantial elliptic flow in RHIC [45]. If the  $J/\psi$  is regenerated, it is expected to inherit this elliptic flow. On the other hand, a color singlet  $J/\psi$  moving through the plasma will not show a substantial flow. While no significant elliptic flow of

$J/\psi$  was seen in RHIC, elliptic flow has been measured in LHC [49] and has been used to argue for substantial regeneration of  $J/\psi$  in the fireball created in LHC [50].

Due to the large mass of the  $b$ , regeneration is usually considered to play a small role in the bottomonia sector. It has, however, been pointed out that the ratio of the different  $\Upsilon(nS)$  states can be explained by regeneration, assuming a  $T_{\text{fr}} \sim 250$  MeV [51].

### 3.2 Quarkonia in the fireball

To calculate quarkonia production cross-section in the fireball produced in the relativistic heavy ion collisions, e.g., the  $J/\psi$  or  $\Upsilon$  peak in dilepton channel, we need to incorporate the inputs from the previous sections in the framework of the evolution of the fireball. For use of quarkonia as a marker of deconfinement, as originally envisaged by Matsui and Satz [1], one needs to have a theoretical calculation of quarkonia production for a given initial temperature of the plasma. For such a quantitative prediction, we need to have an understanding of the following processes.

- The production of  $\bar{c}c$  pair, possibly in a hard  $gg$  collision.
- Connecting the  $\bar{c}c$  pair to the  $J/\psi$  resonance.
- Fate of the  $J/\psi$  as it moves in the plasma, which is expanding and cooling.
- Fate of other  $\bar{c}c$  resonances which can decay to  $J/\psi$ .
- Possibility of generation of  $J/\psi$  at the freezeout.

Usually the quarkonia yield in  $A$ - $A$  collisions is presented as  $R_{AA}$ , ratio of the yield in  $A$ - $A$  collision with the scaled yield in  $pp$  collision (for the same window of variables like  $p_T, y$  etc):

$$R_{AA}(J/\psi) = \frac{N_{AA}(J/\psi)}{N_{\text{coll}} N_{pp}(J/\psi)} \quad (21)$$

where  $N_{\text{coll}}$  is the number of binary collisions. A deviation of  $R_{AA}$  from 1 does not necessarily indicate medium effect. The production of the  $\bar{c}c$  is a hard process; but the gluon distribution function is a nonperturbative input. These distribution functions can be different in the nucleus from that in the proton; e.g., the low  $x$  rise of the gluon distribution function can be tempered due to two low  $x$  gluons fusing (“shadowing”). Usually one extracts the distribution functions in nucleus from inputs like deep inelastic  $e$ - $A$  collisions as well as observables like dilepton and pion production in  $p$ - $A$  collisions [52].

The conversion of the  $\bar{c}c$  to  $J/\psi$  is a complicated process even in the vacuum [53]. Many calculations use the simple “color evaporation model”, where production cross-section of the  $J/\psi$  to the  $\bar{c}c$  production cross section is given simply as

$$\sigma_{J/\psi}(s) \approx g_{\bar{c}c \rightarrow J/\psi} \sigma_{\bar{c}c}(s) \quad (22)$$

with  $g_{\bar{c}c \rightarrow J/\psi}$  energy independent [54]. Similar relations are written for the other charmonia. A more rigorous approach is to use nonrelativistic QCD (NRQCD) [55]. One uses a separation of the scales  $m_Q$  and  $m_Q v$  to write down the  $J/\psi$  as a superposition of a singlet  $\bar{c}c$  state and states where  $\bar{c}c$  are in an octet configuration, combining with  $g$  to form a color singlet. The original  $\bar{c}c$  can form in either color singlet or color octet, and then evolves into the  $J/\psi$  by emitting gluons. If we estimate the formation time of the  $J/\psi$  as  $\tau_{J/\psi} \sim 1/E_b$ , the binding energy of the  $\bar{c}c$  pair, we get  $\tau_{J/\psi} \sim 0.5$  fm, which is of the

order of the formation time of the plasma. For  $J/\psi$  with large  $p_T$ , time dilation increases the formation time further. So the in-medium behavior of the precursor to  $J/\psi$  needs to be understood [56, 57]. In particular, for large  $p_T$   $J/\psi$  the precursor is mostly in color octet state, and it has been argued that it interacts much more readily with the medium, leading to dissolution [42, 56] or quenching of  $p_T$  [57].

The interaction of the  $J/\psi$  (and other quarkonia, which may decay into  $J/\psi$ ) with the medium is probably the most studied part of the scheme outlined above. Following the original intuitive argument of Matsui and Satz [1], many early works used a dissociation temperature, usually from using the singlet free energy in the Schrödinger equation. In a series of papers, Kharzeev and Satz studied the dissociation of the  $J/\psi$  (and its precursor, the color octet state) through gluon dissociation, generalizing the multipole analysis [58] for thermal gluons. For thermal gluons a free gluon gas distribution has been used, which is probably not a good approximation at temperatures of interest to RHIC and LHC. A similar approach has been followed in Ref. [57].

Ideally, the temperature modification of  $J/\psi$  and  $\Upsilon$  should be incorporated by putting in the corresponding spectral function. That is, however, more difficult; what has been done in Refs. [59, 60] is to use the imaginary part of the potential to calculate a thermal decay width, and evolve that through the history of the plasma to calculate a suppression factor  $R_{AA}$ . On the other hand, in Ref. [61] the decay width is obtained from the imaginary part of the quark propagator, which incorporates the scattering T matrix, which can be evaluated self-consistently through a Bethe-salpeter equation [62]. The  $\bar{Q}Q$  potential is an input in the Bethe-Salpeter equation.

It is worth mentioning here that in many studies, the real part of the potential is replaced by an “internal energy” [63], which is obtained by subtracting an entropy term from the singlet free energy, Eq. (11). This has largely been motivated by the fact that use of the free energy seems to give too large a suppression for both  $J/\psi$  and  $\Upsilon(1S)$ . As the discussion in Sec. 2.2 shows, however, there is little theoretical justification for using such an “internal energy” for study of quarkonia dissociation in plasma.

In order to quantitatively study the  $J/\psi$  peak, it is not enough to study the modification of the  $J/\psi$  in the plasma. Almost half of the  $J/\psi$  seen in a  $pp$  collision come from a “feeddown” route: the original  $\bar{c}c$  pair goes to  $\chi$  and  $\psi(2s)$  states, which have a substantial branching fraction to  $J/\psi$ . Some  $J/\psi$  also come from decays of the  $B$  mesons: at Tevatron, this fraction has been estimated as  $\sim 9 \pm 1\%$  [64]. The time scale for the  $B \rightarrow J/\psi$  decay is  $ps$ , and the  $J/\psi$  coming from  $B$  can be subtracted out; the  $J/\psi$  yield after such a subtraction is referred to as “prompt”  $J/\psi$  [64, 65]. Time scales for the feed-down decays from  $\chi_c$  and  $\psi'$  are  $\sim 200$  fm or more. So these states are expected to move through the medium as the excited states. The fraction of  $J/\psi$  coming from  $\psi'$  and  $\chi_c$  states have been estimated as  $\sim 9 \pm 3\%$  and  $\sim 30 \pm 7\%$  at Tevatron, and similar values at lower energies [66]. For the  $\Upsilon(1S)$ , the CDF collaboration has measured the feeddown fraction in Tevatron [67]: for  $p_T > 8$  GeV, the fraction of directly produced  $\Upsilon(1S)$  is about  $51 \pm 12\%$ , while about  $11 \pm 8\%$  come from decay of excited  $\Upsilon$  and  $38 \pm 9\%$  come from  $\chi_b$  decays. Since the excited  $\chi$  or  $\psi'$  states are more readily dissolved by the medium [2, 3, 7, 56], about 50% suppression of the  $J/\psi$  and  $\Upsilon(1S)$  yield can come simply from the melting of the excited states in medium into open charm.

#### 4. Experimental results

There has been an immense body of experimental results on  $J/\psi$  and  $\Upsilon$ , starting from the early experimental efforts to create quark-gluon plasma. For completeness we mention

some trends from the experiments; detailed survey of experimental results can be found elsewhere [68, 69].

$J/\psi$  suppression compared to  $pp$  collisions was already seen at the O-Cu and S-U collisions in the NA38/NA50 experiments in SPS, CERN. However, this suppression could be completely understood in terms of cold nuclear matter effect, like shadowing (Sec. 3.2) and interaction of the  $J/\psi$  with nuclear matter, taking a nuclear absorption cross-section  $\sigma_{J/\psi N}^{\text{abs}} \approx 4$  mb and  $\sigma_{\psi' N}^{\text{abs}} \approx 7$  mb [70]. The investigation of cold nuclear matter effects can be done by conducting  $pA$  collisions at the same energy. This has now become a staple of the experimental program, and understanding the quarkonia yield in such collisions is vital before one can interpret the suppression in  $AA$  collision.

A larger suppression of the  $J/\psi$  than what could be explained by cold nuclear matter effects was observed by the NA50 experiment in 158 A GeV Pb-Pb collisions in SPS. This suggested an onset of deconfinement [4]. A large suppression has also been seen in the 200 A GeV Au-Au collisions in RHIC (Fig. 4). The level of suppression seen was somewhat similar to that seen in SPS, which was a surprise, given the much larger center-of-mass energy and the expectation of a much longer living plasma. One way to explain the data was to assume that in both experiments the plasma was hot enough to dissolve the excited  $\chi_c$  and  $\psi'$  states, but not hot enough to melt the directly produced  $J/\psi$  [71]. The data could also be explained in other ways: e.g., it is possible that a larger part of the directly produced  $J/\psi$  was dissolved in the RHIC experiment, but there was some  $J/\psi$  produced via recombination (Sec. 3.1), to keep the total yield similar [72]. Other attempts to explain the total yield have used only regeneration [42]. As explained in Sec. 3.1, regeneration calculations have been fairly successful in describing the rapidity dependence of the  $J/\psi$  suppression, but have had difficulty explaining the  $p_T$  dependence [73, 74].

The data from the Pb-Pb collisions at much larger center-of-mass energy 2.76 A TeV (but in the forward rapidity region), as measured by the Alice collaboration [75], is also shown in Fig. 4. The data does not show a much stronger suppression. Data at midrapidity, but larger  $p_T$ , from CMS [65] shows suppression at levels similar to the Phenix data in Fig. 4. A combination of suppression and recombination have been suggested to explain the data [76]. However, details of the  $p$ -Pb data for charmonia have not been completely understood [68, 77].

An interesting suggestion has been to look at not the  $R_{AA}$  but the ratio of  $J/\psi$  with open charm cross-section [78, 79]. This will remove the uncertainties due to the nuclear distribution functions. The double ratio [79]

$$S_{J/\psi} = \frac{g_{\bar{c}c \rightarrow J/\psi}^{AA}}{g_{\bar{c}c \rightarrow J/\psi}^{pp}}, \quad g_{\bar{c}c \rightarrow J/\psi} = \frac{N(J/\psi)}{N(\bar{c}c)} \quad (23)$$

then shows the medium modification of  $J/\psi$  binding. Using this quantity, Satz has claimed that the forward rapidity / large  $p_T$  data of LHC does not show any anomalous suppression of  $J/\psi$ , while the RHIC data in Fig. 4 does [79].

A very beautiful measurement of the  $\Upsilon$  production from the CMS experiment avoids many of the experimental uncertainties, and offers a way of studying  $\Upsilon$  suppression in the Pb-Pb collisions in LHC. The right panel in Fig. 4 shows the  $\Upsilon$  peaks in the dimuon channel, where the  $\Upsilon(1S)$  peak has been normalized to agree with the peak in  $pp$  collisions. Then the peaks for the  $\Upsilon(2S)$  and  $\Upsilon(3S)$  are considerably suppressed. In fact, the  $R_{AA}$  value for  $\Upsilon(1S)$  is quoted as  $0.56 \pm 0.08 \pm 0.07$  [80]. From the discussion at the end of Sec. 3.2, this is consistent with no suppression of the direct  $\Upsilon(1S)$  but almost complete suppression of the feeddown component. This is in line with what one would

## Quarkonia in heavy ion collisions

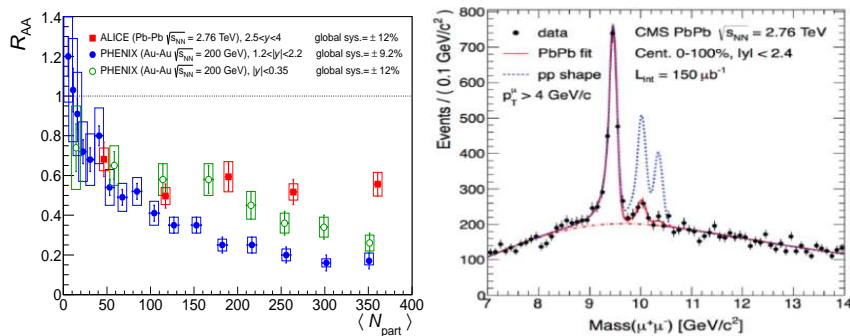


**Figure 4.** (Left)  $J/\psi$   $R_{AA}$  measured by the Alice experiment in the Pb-Pb collisions in LHC at 2.76 A TeV, compared to 200 A GeV Au-Au results from Phenix ([75], ©American Physical Society). (Right)  $\Upsilon$  peaks in the dimuon channel at midrapidity, from CMS [69, 80]. The  $\Upsilon(1S)$  peak has been normalized to the  $pp$  collision, showing the suppression of the  $\Upsilon(2S)$  and  $\Upsilon(3S)$  states.

expect if, following the lattice studies, one expects the  $\Upsilon(1S)$  not to be modified much in the plasma at moderate temperatures, while the excited states melt readily (Sec. 2.1). Note, however, that the large decay widths shown in Fig. 2 would suggest a substantial suppression of the  $\Upsilon(1S)$  also. The  $R_{AA}$  for  $\Upsilon(2S)$  is  $0.12 \pm 0.04 \pm 0.02$  and that for  $\Upsilon(3S)$  is  $< 0.1$  [80], indicating major dissociation of these states.

## 5. Summary and outlook

In this article, the current status of our understanding of quarkonia yield in relativistic heavy-ion collisions is presented. Conceptually, a lot of insight has been gained in the last decade, and the simple picture of quarkonia dissociation due to debye screening has been replaced by a detailed understanding of the dissociation mechanism from QCD.

Lattice QCD (Sec. 2.1) has emerged as a preeminent tool for understanding the behavior of quarkonia in static plasma. But getting quantitative information about the spectral function, decay width etc. have so far been difficult. While it is likely that eventually we will be able to extract the physics from lattice correlators, it probably will require some new ideas. One recent idea has been non-relativistic QCD on lattice, which is a very promising tool for bottomonia at least. Simultaneously, other approaches, largely based on perturbative NRQCD, have clarified many misconceptions (Sec. 2.2). One development has been a theoretically justified construction of a finite temperature effective potential, and illustration of how it captures effects like thermal gluon dissociation.

The calculation of quarkonia yield in the expanding fireball produced in heavy ion collisions is more challenging. In Sec. 3.2 necessary steps are discussed, and some calculations that try to incorporate many of the formal developments of Sec. 2.1 in them are outlined. Of course, for such a calculation one needs to know the behavior of a quarkonium moving with respect to the medium. Some preliminary calculations exist in that direction [81], but clearly more needs to be done. Some other major uncertainties pertain to the formation of the  $J/\psi$ , and interaction of the medium with the precursor to the  $J/\psi$ .

Almost three decades after the suggestion of quarkonia as a probe of the deconfined medium, it remains a topic of great interest. While still not a thermometer of the plasma as originally envisaged by Satz and others [2], it has been an invaluable source of insight

into the nature of the deconfined medium.

### Acknowledgments

I would like to thank Mikko Laine and Jon-Ivar Skullerud for providing me with data related to Figs. 2, 3. The first draft of this article was completed during Whepp-13. I would like to acknowledge discussions with the participants of the meeting, in particular with D. Das, S. Gupta, R. Gavai, R. Sharma, P. Shukla and K. Sridhar.

### References

- [1] T. Matsui and H. Satz, Phys. Lett. B 178 (1986) 416.
- [2] F. Karsch, M.T. Mehr and H. Satz, Z. Phys. C 37 (1988) 617.
- [3] S. Digal, P. Petreczky and H. Satz, Phys.Rev. D64 (2001) 094015.
- [4] M.C. abreu, et al. (NA50 Coll.), Phys. Lett. B 477 (2000) 28.
- [5] M. Le Bellac, *Thermal Field Theory* (Cambridge University Press, 1996).
- [6] See. e.g., O. Philipsen, Prog.Part.Nucl.Phys. 70 (2013) 55; P. Petreczky, J.Phys. G39 (2012) 093002.
- [7] S.Datta, F. Karsch, P. Petreczky and I. Wetzorke, Nucl. Phys. Proc. Suppl. 119 (2003) 487; Phys. Rev. D 69 (2004) 094507.
- [8] K. Nomura, O. Miyamura, T. Umeda and H. Matsufuru, Nucl.Phys.Proc.Suppl. 119 (2003) 496. T. Umeda, H. Matsufuru, K. Nomura, Eur.Phys.J. C39S1 (2005) 9.
- [9] M. Asakawa and T. Hatsuda, Phys. Rev. Lett. 92 (2004) 012001.
- [10] M. Jarrell and J.E. Gubernatis, Phys. Rep. 269 (1996) 133.  
M. Asakawa and T. Hatsuda, Prog. Part. Nucl. Phys. 46 (2001) 459.
- [11] R.K. Bryan, Eur. Biophys. J. 18 (1990) 165.
- [12] W. Press, S. Teukolsky, W. Vetterling and B. Flannery, *Numerical Recipes* (Cambridge University Press, 1989).
- [13] A. Jakovac, P. Petreczky, K. Petrov and A. Velytsky, Phys.Rev. D75 (2007) 014506.
- [14] G. Aarts, et al., Phys.Rev. D76 (2007) 094513.  
M. Oktay and J-I. Skullerud, arxiv:1005.1209.
- [15] S. Borsanyi, et al., J. High energy Physics. 1404 (2014) 132.
- [16] T. Umeda, Phys.Rev. D75 (2007) 094502.
- [17] S. Datta and P. Petreczky, J.Phys. G35 (2008) 104114.  
P. Petreczky, Eur.Phys.J. C62 (2009) 85.
- [18] A. Mocsy and P. Petreczky, Eur.Phys.J.ST 155 (2008) 101. Phys.Rev.Lett. 99 (2007) 211602
- [19] H.T. Ding, et al., Phys.Rev. D86 (2012) 014509.
- [20] G. Aarts, et al., JHEP 1111 (2011) 103.
- [21] G. Aarts, et al., JHEP 1312 (2013) 064.
- [22] G.P. Lepage, et al., Phys. Rev. D 46 (1992) 4052.
- [23] S. Datta, A. Jakovac, F. Karsch and P. Petreczky, AIP Conf.Proc. 842 (2006) 35.
- [24] N. Brambilla, M. Escobedo, J. Ghiglieri, J. Soto and A. Vairo, JHEP 1009 (2010) 038.
- [25] S. Kim, P. Petreczky and A. Rothkopf, PoS Lattice 2013 (2014) 169.
- [26] L. McLerran and B. Svetitsky, Phys. Rev. D 24 (1981) 450.
- [27] S. Nadkarni, Phys. Rev. D 34 (1986) 3904.
- [28] O. Kaczmarek, F. Karsch, P. Petreczky and F. Zantow, Phys. Lett. B 543 (2002) 41.  
O. Kaczmarek and F. Zantow, Phys.Rev. D71 (2005) 114510.
- [29] M. Laine, O. Philipsen, P. Romatschke and M. Tassler, JHEP 0703 (2007) 054.
- [30] N. Brambilla, J. Ghiglieri, A. Vairo and P. Petreczky, Phys. Rev. D78 (2008) 014017.
- [31] A. Beraudo, J-P. Blaizot and C. Ratti, Nucl. Phys. A 806 (2008) 312.
- [32] For a review, see N. Brambilla, A. Pineda, J. Soto and A. Vairo, Rev. Mod. Phys. 77 (2005) 1423.
- [33] R.D. Pisarski, Phys. Rev. Lett. 63 (1989) 1129.



*Quarkonia in heavy ion collisions*

- [34] N. Brambilla, M. Escobedo, J. Ghiglieri and A. Vairo, JHEP 1112 (2011) 116.
- [35] C. Young and K. Dusling, Phys. Rev. C 87 (2013) 065206.  
N. Borghini and C. Gombeaud, Eur. Phys. J. C 72 (2012) 2000.  
Y. Akamatsu and A. Rothkopf, Phys. Rev. D 85 (2012) 105011.
- [36] Y. Akamatsu, Phys. Rev. D 87 (2013) 045016.
- [37] Y. Burnier and A. Rothkopf, Phys. Rev. D 87 (2013) 114019.
- [38] Y. Burnier and A. Rothkopf, Phys. Rev. Lett. 111 (2013) 182003.
- [39] Y. Burnier, M. Laine and M. Vepsalainen, JHEP 0801 (2008) 043.
- [40] P. Petreczky, C. Miao and A. Mocsy, Nucl.Phys. A855 (2011) 125.
- [41] P. Braun-Munzinger and J. Stachel, Phys. Lett. B 490 (2000) 196.  
R.L. Thews, M. Schroedter and J. Rafelski, Phys. Rev. C 63 (2001) 054905.
- [42] A. Andronic, P. Braun-Munzinger, K. Redlich and J. Stachel, Nucl. Phys. A 789 (2007) 334.
- [43] C. Young and E. Shuryak, Phys. Rev. C 79 (2009) 034907.
- [44] G.D. Moore and D. Teaney, Phys. Rev. C 71 (2005) 064904.
- [45] A. Adare, et al. (PHENIX Coll.), Phys. Rev. C 84 (2011) 044905.
- [46] A. Francis, O. Kaczmarek, M. Laine and J. Langelage, PoS Lattice2011 (2011) 202.  
D. Banerjee, S. Datta, R. Gavai and P. Majumdar, Phys. Rev. D 85 (2012) 014510.
- [47] L. Grandchamp and R. Rapp, Nucl. Phys. A 715 (2003) 545.
- [48] L. Yan, P. Zhuang, and N. Xu, Phys. Rev. Lett. 97 (2006) 232301.
- [49] E. Abbas, et al. (ALICE Coll.), Phys. Rev. Lett. 111 (2013) 162301.
- [50] X. Zhao, A. Emerick and R. Rapp, Nucl. Phys. A 904-905 (2013) 611c.
- [51] S. Gupta and R. Sharma, Phys. Rev. C 89 (2014) 057901.
- [52] See K.J. Eskola, H. Paukkunena and C.A. Salgado, JHEP 0904 (2009) 065, for a recent estimate of the nuclear distribution functions.
- [53] N. Brambilla, et al. (Quarkonium Working Group), “*Heavy quarkonium physics*”, CERN Report (hep-ph/0412158).
- [54] R. Gavai, et al., Int. J. Mod. Phys. A10 (1995) 3043.
- [55] G.T. Bodwin, E. Braaten, and G.P. Lepage, Phys. Rev. D 51 (1995) 1125.
- [56] D. Kharzeev and H. Satz, Phys. Lett. B 334 (1994) 155.  
X. Xu, D. Kharzeev, H. Satz and X. Wang, Phys. Rev. C 53 (1996) 3051.
- [57] R. Sharma and I. Vitev, Phys. Rev. C 87 (2013) 044905.
- [58] G. Bhanot and M. Peskin, Nucl.Phys. B156 (1979) 391.
- [59] M. strickland and D. Bazow, Nucl. Phys. A 879 (2012) 25.
- [60] M. Margotta, et al., Phys. Rev. D 83 (2011) 105019.
- [61] F. Riek and R. Rapp, New J. Phys. 13 (2011) 045007.
- [62] M. Mannarelli and R. Rapp, Phys. Rev. C 72 (2005) 064905.  
D. Cabrera and R. Rapp, Phys. Rev. D 76 (2007) 114506.
- [63] O. Kaczmarek, F. Karsch, P. Petreczky and F. Zantow, Nucl.Phys.Proc.Suppl. 129 (2004) 560.  
O. Kaczmarek and F. Zantow, Eur.Phys.J. C43 (2005) 59.
- [64] D. Acosta et al. (CDF Coll.), Phys.Rev. D71 (2005) 032001.
- [65] S. Chatrchyan, et al. (CMS Coll.), JHEP 05 (2012) 063.
- [66] P. Faccioli, C. Lourenco, J. Seixas and H. Woehri, JHEP 0810 (2008) 004.  
F. Abe et al. (CDF Coll.), Phys. Rev. Lett. 79 (2003) 578.
- [67] T. Affolder, et al., Phys.Rev.Lett. 84 (2000) 2094.
- [68] D. Das, Conf.Proc. 57 (2012) 37-44 (Proceedings, DAE Symposium on Nuclear Physics, 2012; arXiv:1212.2704.) A. Rossi, EPJ Web Conf. 60 (2013) 03003 (Proceedings of the LHCP conference; arXiv:1308.2973).
- [69] I. Tserruya, Proceedings, “New Trends in High Energy Physics” (arXiv:1311.4456).
- [70] B. Alessandro, et al. (NA50 Coll.), Phys. Lett. B 553 (2003) 167; Eur. Phys. J. C 33 (2004) 31.
- [71] F. Karsch, D. Kharzeev and H. Satz, Phys. Lett. B 637 (2006) 76.
- [72] X. Zhao and R. Rapp, Phys. Lett. B 664 (2008) 253.
- [73] A. Adare et al. (PHENIX Coll.), Phys. Rev. Lett. 98 (2007) 232301.
- [74] A. Adare et al. (PHENIX Coll.), Phys. Rev. C 84 (2011) 054912.

*S. Datta*

- [75] B. Abelev, et al. (ALICE Coll.), Phys. Rev. Lett. 109 (2012) 072301.
- [76] X. Zhao and R. Rapp, Nucl. Phys. A 859 (2011) 114.
- [77] B. Abelev, et al. (ALICE Coll.), JHEP 1402 (2014) 073.  
L. Manceau, EPJ Web Conf. 60 (2013) 13002 (Proceedings of the LHCP conference; arXiv:1307.3098).
- [78] K. Sridhar and H. Satz, Phys. Rev. D 50 (1994) 3557.
- [79] H. Satz, Adv. High Energy Physics. 2013 (2013) 242918.
- [80] S. Chatrchyan, et al., Phys. Rev. Lett. 109 (2012) 222301.
- [81] S. Datta, et al., in: proceedings, Strong and Electroweak Matter 2004, Helsinki, Finland (arXiv:hep-lat/0409107). G. Aarts, et al., Nucl. Phys. A 785 (2007) 1c (Proceedings, Strong and Electroweak Matter 2006, Brookhaven, USA). S. Kim, et al., PoS LATTICE2012 (2012) 086.